Exploration of New Chromophore Structures Leads to the Identification of Improved Blue Fluorescent Proteins†

Hui-wang Ai,‡ Nathan C. Shaner,§,|| Zihao Cheng,‡ Roger Y. Tsien,§ and Robert E. Campbell*,‡

University of Alberta, Department of Chemistry, Edmonton, Alberta, Canada T6G 2G2, and Departments of Pharmacology and Chemistry, Howard Hughes Medical Institute, University of California at San Diego, 9500 Gilman Drive, La Jolla, California 92093

Received January 30, 2007; Revised Manuscript Received March 2, 2007

ABSTRACT: The variant of *Aequorea* green fluorescent protein (GFP) known as blue fluorescent protein (BFP) was originally engineered by substituting histidine for tyrosine in the chromophore precursor sequence. Herein we report improved versions of BFP along with a variety of engineered fluorescent protein variants with novel and distinct chromophore structures that all share the property of a blue fluorescent hue. The two most intriguing of the new variants are a version of GFP in which the chromophore does not undergo excited-state proton transfer and a version of mCherry with a phenylalanine-derived chromophore. All of the new blue fluorescing proteins have been critically assessed for their utility in live cell fluorescent imaging. These new variants should greatly facilitate multicolor fluorescent imaging by legitimizing blue fluorescing proteins as practical and robust members of the fluorescent protein "toolkit".

Fluorescence imaging of protein dynamics in live cells now relies heavily on recombinant genes encoding fluorescent proteins (FPs[1]) cloned from cnidarian marine species (*1*, *2*). Recombinant FP expression vectors are commonplace in biochemical research environments, and anyone with basic molecular biology expertise can rapidly create a FP chimera with their protein of interest. Subsequent imaging of transfected cells with ubiquitous and relatively inexpensive fluorescence microscopy equipment provides insight into the subcellular localization and spatiotemporal dynamics of the protein of interest. While wild-type FP genes can certainly be useful for such applications in and of themselves, they are generally burdened with one or more of the following suboptimal properties: poor folding efficiency at 37 °C, dim fluorescent brightness, oligomeric structure, or poor photostability. Fortunately, protein-engineering efforts have resulted in the creation of variants that retain the same hue, but not the handicaps, of their wild-type precursor and are thus far more suitable for use in live cell fluorescence imaging (*2*).

Certain intrinsic photophysical properties of a FP, such as quantum yield and propensity to photobleach, are necessarily determined both by the covalent structure of the chromophore (Figure 1A−H) and by the interactions of the chromophore with the surrounding amino acid residues. The extinction coefficient depends on these same factors as well as on the folding and chromophore maturation efficiency. A particular challenge facing protein engineers seeking bright new hues of FPs is that the key mutation for creation of a new color necessarily involves a dramatic change in the chromophore structure or environment. This dramatic change typically has severe adverse effects on the protein folding and chromophore formation efficiency. Furthermore, when the covalent structure of the chomophore has been altered by the mutation (i.e., by replacement of Tyr66 with a different aromatic amino acid, refer to Figure 1), the surrounding residues generally require optimization to once again maximize brightness. The growing number of reports in which researchers have significantly modified a FP but then optimized it for its new favorable properties could understandably leave one with the impression that all new colors of FP are readily amenable to improvement (*3*−*5*). However, in our experience we have found that some chromophore structures (e.g., mHoneydew (*6*), Figure 1F) are seemingly more resistant to improvement than others (e.g., mTFP1 (*5*)). This observation led us to question whether certain suboptimal FP variants are limited by the intrinsic properties of their chromophore or by insufficient effort expended in their optimization.

A particularly interesting case study that epitomizes the challenges described in the preceding paragraph is the development of the protein now known as enhanced blue FP (EBFP). Concurrent with the first reports detailing the heterologous and functional expression of the GFP in organisms other than jellyfish (*7*−*9*), researchers were already working to create the GFP variant that would be progenitor of EBFP (*10*). Introduction of the Tyr66His

† This work was supported in part by a grant from the Natural Sciences and Engineering Research Council of Canada (NSERC) and an Alberta Ingenuity New Faculty Award (to R.E.C.). N.C.S. was supported by a Howard Hughes Medical Institute Predoctoral Fellowship.

* To whom correspondence should be addressed. Tel: (780) 492-1849. Fax: (780) 492-8231. E-mail: robert.e.campbell@ualberta.ca.

‡ University of Alberta.

§ University of California, San Diego.

|| Present address: The Salk Institute for Biological Studies, 10010 North Torrey Pines Road, La Jolla, CA 92037.

[1] Abbreviations: FP, fluorescent protein; GFP, wild-type *Aequorea* green FP; BFP, GFP Y66H/Y145F; EBFP, BFP F64L/S65T; EBFP1.2/1.5/2, variants of EBFP; mBlueberry1/2, variants of mCherry Y67F; mKalama1, a blue-fluorescing variant of GFP with a tyrosine-derived chromophore.

10.1021/bi700199g CCC: $37.00
Published on Web 04/20/2007

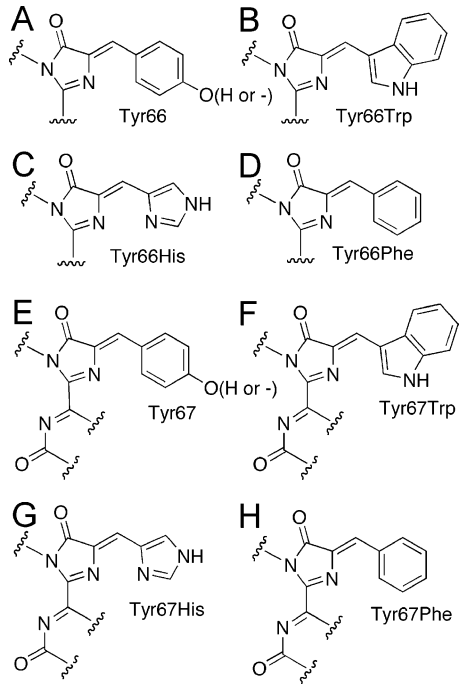

FIGURE 1: Representative covalent structures of chromophores. (A) Wild-type GFP ground state (*24*) and mKalama1 (phenol), EGFP (*25*) and mTFP1 (*5*) (phenolate); (B) ECFP (*10*); (C) EBFP variants; (D) GFP-Y66F; (E) Keima ground state (*26*) (phenol), DsRed (*22*) and most mFruit variants (*6*) (phenolate); (F) mHoneydew (*6*); (G) mCherry2-Y67His; and (H) mBlueberry variants. Although they are not represented in this figure, noncovalent interactions between the protein and the chromophore (e.g., the cationic imidazole ring of His197 in mTFP1 (*5*)) are also important determinants of the fluorescence hue.

mutation (Figure 1C) into wild-type GFP (excitation maxima at 395 and 475 nm and emission maximum at 508 nm) produced a variant with a fluorescence emission wavelength substantially blue-shifted (excitation maximum at 383 nm and an emission maximum at 447 nm) from that of the wild-type protein (*10*). As might be expected for such a radical change in the chromophore structure, the resulting protein had a relatively poor extinction coefficient (ϵ) of 13 500 M^{-1} cm^{-1} and quantum yield (ϕ) of 0.21. In the first reported effort to improve the brightness, screening of $\sim 10^4$ colonies expressing randomly mutated versions of the Tyr66His variant was sufficient for the identification of the 2-fold brighter Y66H/Y145F double mutant (*3*) which was designated blue fluorescent protein (BFP). The utility of BFP was further improved by introducing these two mutations into a codon optimized synthetic gene encoding GFP-F64L/S65T (known as enhanced GFP or EGFP) (*11*). The resulting protein, known as EBFP, remained essentially uncontested as the best available example of a blue fluorescing FP until very recently (*12*). Initially, the EBFP/EGFP pair was the only option for dual color imaging and fluorescence resonance energy transfer (FRET) experiments. However, with the advent of the brighter, more photostable, and distinguishable FP hues of cyan (CFP) and yellow (YFP), there was no longer any need for researchers to tolerate the dim fluorescence and fast photobleaching of the EBFP half of the EBFP/EGFP pair. The relevance of EBFP has been further diminished by the relatively recent and explosive growth in the availability of red hues of FPs, most notably the mFruit series of variants (*6*). The mFruit series provides a number of new distinguishable colors that can be paired with EGFP for 2-color imaging or FRET, or with CFP and YFP for 3-color imaging.

A bright and reasonably photostable FP with fluorescence at ~450 nm has long remained a conspicuous absence from the selection of FPs that are recommended for use in live cell imaging (*2*). However, this situation appears to have changed with the recent report of Azurite, a new BFP isolated from a computationally designed library by flow cytometry (*12*, *13*). The photostability of Azurite is improved 40-fold relative to BFP, putting Azurite on par with some of the less photostable of the more popular and practical FPs commonly used in live cell imaging (*2*). It is reasonable to expect that Azurite will find widespread use as a distinct third color (e.g., when used in combination with EGFP and mCherry) in cytometry and fluorescence imaging applications. However, blue fluorescent variants with further improvements in both brightness and photostability would be desirable.

In our own efforts to develop a superior alternative to EBFP we have investigated the potential utility of a variety of alternative blue-fluorescing FPs with chemically distinct chromophore structures. Herein we describe the creation of a variety of novel FPs including a blue-fluorescing variant of GFP with a tyrosine-derived chromophore, improved versions of EBFP, and blue-fluorescing variants of *Discosoma* red FP (RFP). These efforts have resulted in the creation of variants that are both brighter and more photostable than Azurite. The usefulness of our new BFPs in fluorescence imaging applications is compared, and recommendations are made.

MATERIALS AND METHODS

General Methods. All routine molecular biology procedures were carried out as previously described (*5*). Synthetic DNA oligonucleotides for cloning and library construction were purchased from Integrated DNA Technologies (Coralville, IA). PCR products and products of restriction digests were routinely purified using the QIAquick PCR purification kit (Qiagen) according to the manufacturer's protocols. Restriction endonucleases were purchased from either Invitrogen or New England Biolabs. The cDNA sequences for all FP variants and fusion constructs were confirmed by dye terminator cycle sequencing using the DYEnamic ET kit (Amersham Biosciences). Sequencing reactions were analyzed at the University of Alberta Molecular Biology Service Unit. All filters for fluorescence screening and imaging were purchased from Chroma Technology (Rockingham, VT).

Library Construction and Mutagenesis. Gene libraries with saturation mutagenesis at a particular residue and libraries of randomly mutated genes were constructed as previously described (*5*). PCR products were digested with *Xho*I and *Eco*R1 and ligated into similarly digested pBAD/HisB vector (Invitrogen). Electrocompetent *Escherichia coli* strain DH10B (Invitrogen) was transformed and plated on Luria−Bertani (LB)/agar plates supplemented with ampicillin (0.1 mg/mL) and L-arabinose (0.02%). Plates were incubated for 14 h at 37 °C prior to screening. To create the gene encoding Azurite (*12*), site-directed mutagenesis was used to introduce the T65S (reversion to wild type), V150I, and V224R mutations in EBFP.

Screening. The screening system has been described previously (*14*). Briefly, the light from a 175W xenon-arc lamp (Sutter) is passed through a 375 to 415 nm bandpass filter and into a bifurcated fiber optic bundle (Newport). Light exiting the fiber optic bundle illuminates a 10 cm dish placed in a recessed holder on the bench top. Colony fluorescence was screened by imaging with a Retiga 1300i 12-bit CCD camera (QImaging) fitted with a 440 to 480 nm bandpass filter. A 500 to 520 nm bandpass filter was used to measure GFP channel signal during ratiometric screening.

Colonies with more intense fluorescence or higher blue/green ratio were picked and cultured overnight in 4 mL of LB medium containing ampicillin and arabinose. The following day 0.1 mL of each culture was dispensed into a 96-well plate (Nunc) and the full emission spectra of each variant measured with a Safire2 plate reader (Tecan). Variants with the most blue-shifted and/or intense emission peak were used as templates in the subsequent round of library construction.

Protein Purification. E. coli strain LMG194 was transformed with the pBAD/His B expression vector containing the FP gene of interest. A single colony was used to inoculate a 4 mL culture that was allowed to grow overnight (37 °C, 225 rpm) before being diluted into 1 L of LB medium containing ampicillin (0.1 mg/mL) and L-arabinose (0.2%). The culture was allowed to grow for 12 h before cells were harvested by centrifugation and lysed by French Press. Proteins were purified by Ni-NTA chromatography (Amersham).

Protein Characterization. Absorption spectra were recorded on a DU-800 UV−visible spectrophotometer (Beckman). A QuantaMaster spectrofluorometer (Photon Technology International) was used to acquire the fluorescent excitation and emission spectra. Quantum yields for all blue FP variants were measured using quinine sulfate in 0.1 M H_2SO_4 as the reference standard (*15*). Protein concentrations used in the calculation of extinction coefficients were determined by the BCA method (Pierce). For fluorescence pK_a measurements, the protein of interest was first dialyzed into dilute buffer (5 mM Tris HCl, pH 7.5) before dilution into a series of 200 mM buffers. Fluorescent intensity was measured using a fluorescence plate reader equipped with monochromators (Tecan).

Photostability measurements were performed essentially as previously described (*2*, *5*). Briefly, microdroplets of each blue FP were generated by vortexing the protein solution (100 μM) with mineral oil. Approximately 5 μL of this suspension was sandwiched between a glass slide and a glass cover slip. Single drops were identified at low light levels (2.5% neutral density filters) on a wide-field microscopy instrument equipped with a 75 W HBO lamp. Neutral density filters were removed, and the protein drop was imaged with a 50 ms exposure time and without closing the shutter. Typical frame rates were 1 image/s, though it was necessary to go as fast as 3 images/s for the fast bleaching proteins and as slow as 0.03 image/s for the slow bleaching proteins. Bleaching curves were normalized to the photon emission rate of 1000 photon/s/molecule at the starting time. For all experiments, T-Sapphire (*2*, *16*) was subjected to bleaching under identical conditions and used as a reference standard.

Live Cell Imaging. To create the nuclear localization plasmid for mammalian expression, the gene encoding each blue FP was PCR amplified with a 5′ primer encoding an *Nhe*I site and a 3′ primer encoding an *Xho*I site. The purified and digested PCR product was ligated into the pEYFP-Nuc vector (Clontech) digested with the same restriction enzymes. DNA was purified by Plasmid Midi kit (Qiagen). HeLa cells in 35 mm imaging dishes were transfected with 2 μg of plasmid DNA encoding the blue FP and 2 μg of pEGFP-Actin (Clontech). Cells were treated with the DNA mixed with 10 μg of PEI in 0.5 mL of OptiMEM (Invitrogen), and serum was added after 30 min. The next day the medium was exchanged for PBS and the cells were imaged on an Axiovert 200M (Zeiss) equipped with a 75 W xenon-arc lamp. Blue fluorescence was imaged using a 375 to 415 nm bandpass excitation filter, a 425 nm long-pass beamsplitter, and a 440 to 480 nm bandpass emission filter. Green fluorescence was imaged using a 450 to 490 nm bandpass excitation filter, a 495 nm long-pass beamsplitter, and a 500 to 550 nm bandpass emission filter.

RESULTS

Aequorea GFP Variants with a Tyrosine-Derived Chromophore. GFP S65G/S72A/T203F (denoted T203F) is a yellow fluorescing GFP variant that has a strong absorption peak at 510 nm and a weak absorption peak at 405 nm (*17*). By analogy with wild-type GFP (with absorption peaks at 475 and 396 nm), the species that gives rise to the two absorption peaks of T203F is an equilibrating mixture of the lower energy anionic phenolate and higher energy neutral phenol forms of the chromophore, respectively. If wild-type GFP is excited at either absorbance peak, a single fluorescence emission peak, attributable to the excited state of the anionic chromophore, is observed at 508 nm. In contrast, excitation of the T203F variant at the 405 nm peak produces a fluorescence peak at 455 nm while excitation at the 510 nm peak produces a fluorescence peak at 525 nm. The dramatically different fluorescence peaks resulting from excitation of the nominally identical neutral phenol chomophores of wild type and T203F is explained by a fast excited-state protein transfer (ESPT) that occurs in wild type but not in T203F. PS-CFP, a photoswitchable variant of a GFP homologue from *Aequorea coerulescens* (*18*), does not undergo ESPT prior to photoactivation.

It occurred to us that a non-photoswitchable variant of GFP that existed solely in the neutral phenol form in the ground state and that was incapable of ESPT would be a promising alternative to EBFP. With EGFP as our template, we created an initial gene library of ~4000 variants in which Thr65 was mutated to all amino acids and an additional 3 residues in close proximity to the chromophore (His148, Thr203, and Ser205) were simultaneously mutated to a subset of hydrophobic residues. Fluorescence imaging-based screening of this library in bacterial colonies was undertaken to find variants with strong blue fluorescence (excitation at 400/20 nm and emission 460/40 nm). To screen against variants that existed partially in an anionic phenolate ground state or that were partially capable of ESPT, we performed ratiometric screening for colonies that had high blue fluorescence and low green fluorescence (emission at 525/20 nm when excited with either 400/20 nm or 470/20 nm light). Exhaustive screening of our initial library resulted in the identification of EGFP T65S/H148G/T203V/S205V that exhibited strong

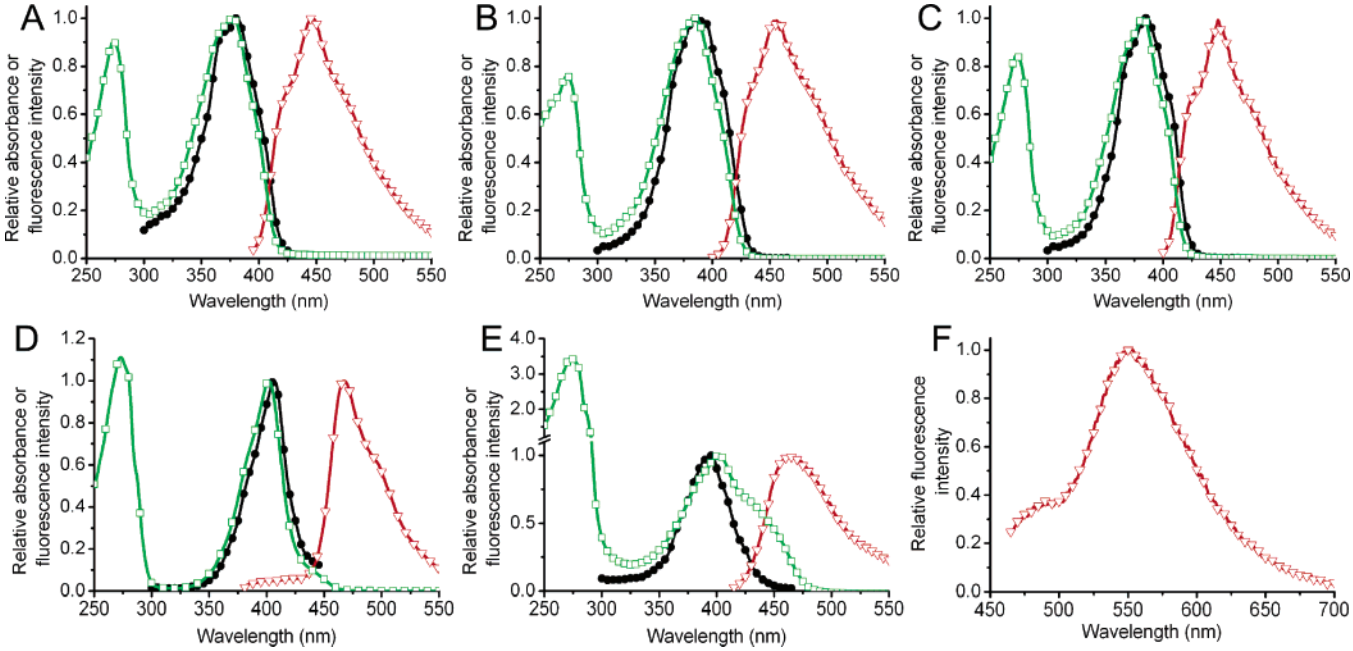

FIGURE 2: Spectral characterization of new variants. Shown in each panel are the absorbance (green), excitation (black), and emission (red) spectra for the indicated protein. (A) EBFP, (B) mKalama1, (C) EBFP2, (D) mBlueberry2, (E) mCherry2-Tyr67His immediately after purification, (F) fluorescence emission spectrum (excitation at 450 nm) for mCherry2-Tyr67His after 1 day at 4 °C.

Table 1: Overview of Mutations in Blue-Fluorescing FPs

protein	mutations
mKalama1	EGFP-L18M/H25R/S30R/E32V/ Y39H/T50S/T65S/N105S/E124V/ I128T/Y145M/S147V/H148G/ M153T/V163A/K166E/I171V/ S175G/P192S/T203V/S205V/ A206K/V224R/L231P
EBFP	EGFP-Y66H/Y145F
EBFP1.2	EBFP-S30R/Y39N/T65S/S72A/ N105T/I171V/N198S/A206V
EBFP1.5	EBFP1.2-F145H/H148N/M153A
EBFP2	EBFP1.2-I128V/V150I/ D155V/ V224R
mBlueberry1	mCherry2-M66L/Y67F/K70R/ Q137R/C138R/Y151C/Q163L/ K168R
mBlueberry2	mCherry2-D6aN/M18V/A57T/ Y67F/A71V/V73I/L83F/N92R/ E117V/S146F/G159S/Q163T/ L202V
Azurite	EBFP-T65S/V150I/V224R

blue fluorescence and essentially no green fluorescence (Figure 2B). Subsequent rounds of both (semi)saturation (positions 30/39/63/64/105/145/147/153/163/171/175/181) and random mutagenesis were undertaken and halted only when no further improvement had been observed for several rounds of screening. The most brightly fluorescent variant discovered during the directed evolution process had 22 mutations relative to EGFP (Table 1). In addition, the "monomerizing" A206K mutation (*19*) and the Azurite-derived V224R mutation (*12*) (discussed below) were introduced by site-directed mutagenesis. We have named the protein mKalama1 after the bright blue waters of Kalamalka lake of southern British Columbia (the preceding "m" denotes the presence of the A206K mutation). mKalama1 (ϵ = 36 000 M^{-1} cm^{-1} and ϕ = 0.45) is 3.6-fold brighter and 25-fold more photostable than EBFP (Table 2).

Improved Versions of Aequorea-Derived EBFP. We had initially presumed that EBFP was close to the maximum achievable fluorescent brightness for its particular chromophore structure (Figure 1C). However, the recent report from Waldo and co-workers (*20*) that introduction of the "superfolder" mutations into BFP improved the fluorescent brightness in bacterial colonies galvanized us to explore whether these mutations could also benefit EBFP. Mutations S30R/Y39N/T65S/S72A/N105T/I171V/N198S/A206V were introduced into EBFP by site-directed mutagenesis to produce EBFP1.2 (EBFP1.2). The fact that EBFP1.2 (ϵ = 41 000 M^{-1} cm^{-1} and ϕ = 0.45) was 4-fold brighter than EBFP caused us to ask whether further improvements might be realized by directed evolution. Starting from the EBFP1.2 template, we undertook several rounds of library creation and screening with particular focus on residues in close proximity to the chromophore. This effort resulted in the identification of EBFP1.2-F145H/H148N/M153A, which was designated EBFP1.5 (ϵ = 43 000 M^{-1} cm^{-1} and ϕ = 0.53).

Azurite is a recently described BFP variant with improved brightness and photostability (*12*). The two key mutations, V150I and V224R, responsible for the favorable properties of Azurite were introduced into both EBFP1.2 and EBFP1.5. Disappointingly, these substitutions greatly diminished the fluorescence of our most highly optimized EBFP1.5 variant. When introduced into EBFP1.2, these substitutions caused only ~30% decrease in brightness but conferred a remarkable increase in photostability. Additional rounds of random mutagenesis and screening recovered the lost brightness to produce EBFP2 (Table 1), a variant that is 4-fold brighter and 550-fold more photostable than EBFP (Table 2). Relative to Azurite, EBFP2 is 1.4-fold brighter and 2.9-fold more photostable. Neither Azurite nor EBFP2 contains the A206K mutation (*19*). Consequently, both proteins may retain wild-type GFP's tendency to dimerize at high concentrations. However, it has been suggested that the A206V "superfolder" mutation of EBFP2 could hinder dimerization (*20*).

Table 2: Properties of New Blue-Fluorescing FPs

parent	protein	λ_{ab} (nm)	λ_{em} (nm)	ϵ[a]	ϕ	brightness[b]	pK_a	photostability (s)[c]
EGFP	mKalama1	385	456	36	0.45	16	5.5	2.5
EBFP	EBFP2	383	448	32	0.56	18	5.3	55
	EBFP1.5	381	449	43	0.53	23	4.8	2.4
	EBFP1.2	379	446	41	0.45	18	6.6	0.95
mCherry	mBlueberry2	402	467	51	0.48	25	<2.5	<0.05
	mBlueberry1	398	452	11	0.48	5	nd[d]	<0.02
	mCherry2-Y67H[e]	402	464	6	0.06	0.3	nd	nd
previous work[f]	Azurite	384	450	22	0.59	13	5.0	19
	EBFP	377	446	30	0.15	4.5	6.3	0.10

[a] Units of mM^{-1} cm^{-1}. [b] Product of ϵ and ϕ in mM^{-1} cm^{-1}. For comparison, the brightness of EGFP is 34 mM^{-1} cm^{-1} (*2*). [c] Time to photobleach from 1000 to 500 photons/s/molecule. [d] Not determined. [e] Wavelength values are given for the initially purified protein. [f] All values measured in this laboratory.

Discosoma RFP Variants. Discosoma RFP (also known as DsRed or dsFP583) is a GFP homologue (*21*) that harbors a chromophore in which the conjugation has been extended through an additional acylimine moiety derived from main chain atoms (Figure 1E) (*22*). The additional conjugation results in a substantial red-shift in the absorbance (558 nm) and fluorescence peaks (583 nm) relative to GFP. Extensive engineering and directed evolution of *Discosoma* RFP has resulted in a series of monomeric variants known as the "mFruits", where each variant is named for a fruit of similar color (*6*). For GFP variants it is known that the series of variants in which Tyr66 is replaced with Trp (Figure 1B), His (Figure 1C), or Phe (Figure 1D) results in new chromophore structures with increasingly blue-shifted absorbance and fluorescence (*1*). A monomeric Tyr67Trp variant known as mHoneydew (Figure 1F) has previously been investigated and shown to have broad yellow fluorescence (*6*).

With the expectation of obtaining further blue-shifted variants we introduced the Tyr67His and Tyr67Phe mutations into the *Discosoma* RFP variant known as mCherry2 (N.C.S. and R.Y.T., unpublished results). The mCherry2-Tyr67Phe variant had absorption (405 nm) and emission peaks (467 nm) (Figure 2D) significantly red-shifted from the GFP-Tyr66Phe (absorption at 360 nm and emission at 442 nm), indicating that this variant was still capable of all post-translational steps necessary for chromophore formation (Figure 1H). Starting from mCherry2-Tyr67Phe, we initiated directed evolution as described above. The resulting protein, which we have named mBlueberry1 (Table 1), as it is a new member of the mFruit series, has a very good quantum yield ($\phi = 0.48$) but a disappointingly low extinction coefficient ($\epsilon = 11\,000$ M^{-1} cm^{-1}) (Table 2). In the hopes that an alternative template would be more amenable to improvement, we introduced the Tyr67Phe mutation into mApple, a recent addition to the mFruit series that was derived from mCherry2 (N.C.S. and R.Y.T., unpublished results). Directed evolution of this variant resulted in the creation of mBlueberry2 (Table 1), which is 4.6-fold brighter than mBlueberry1 (Table 2). For the sake of consistency, mutations in both mBlueberry1 and mBlueberry2 are listed in Table 1 relative to their common ancestor, mCherry2. The higher brightness of mBlueberry2 relative to mBlueberry1 is attributed to improvements in extinction coefficient ($\epsilon = 51\,000$ M^{-1} cm^{-1}). A particularly interesting feature of mBlueberry2 is that its fluorescent intensity is unchanged over pH values ranging from less than 2.5 to greater than 10 (Table 2).

By analogy with GFP variants, we expected the mCherry2-Tyr67His mutant to have a fluorescent hue intermediate between mHoneydew and mBlueberry. The freshly purified protein has a fluorescence peak at 464 nm when excited at 400 nm. However, within 24 h of being purified, a new minor absorbance peak at 450 nm becomes apparent. Excitation of this peak produces an unexpectedly long wavelength fluorescence emission peak at 550 nm (Figure 2F). Unfortunately this intriguing protein stubbornly resisted improvement by directed evolution with selection for mutants with improved brightness at either the 464 nm or 550 nm emission peaks. It has previously been shown that the isolated BFP chromophore has a pK_a of 12.0 for formation of its red-shifted anionic form (*23*). The acylimine extension off the mCherry2-Tyr67His chromophore should enable greater delocalization of the negative charge and may thereby cause a significant decrease in the pK_a. We tentatively speculate that the 550 nm peak may arise from the anionic form of the histidine-derived chromophore. Alternatively, the chromophore may be undergoing an additional post-translational modification that extends the conjugation.

DISCUSSION

Intrinsic fluorescent brightness is, ostensibly, the most obvious characteristic by which to compare FPs. By this criterion, four of the new FPs (EBFP1.5, EBFP2, mKalama1, and mBlueberry2) and the recently reported Azurite variant (*12*) are all significantly improved relative to EBFP. The brightest of the new variants is mBlueberry2, followed closely by EBFP1.5. However, it is important to note that the primary limitation of EBFP was not its brightness but rather its susceptibility to photobleaching. We determined the rates of photobleaching (*2*) for each of the new variants in microdrops of purified protein (Figure 3). Unfortunately, the brightest variant, mBlueberry2, was notable for a remarkably fast rate of photobleaching that was comparable with EBFP. At light intensities that would typically be used for widefield fluorescence imaging, the fluorescence of mBlueberry2 (and mBlueberry1) decreased to less than 20% in less than 100 ms of total exposure time. This characteristic renders mBlueberry2 impractical for use in routine imaging experiments but is intriguing with regard to future studies of the mechanism of chromophore bleaching. In contrast, the other 3 new variants exhibited rates of photobleaching that were significantly improved relative to EBFP. The most spectacular improvements were observed with EBFP2, which exhibits a 550-fold improvement in photostability relative to EBFP. These benefits stem from the presence of the V150I and V224R mutations to which the similarly impressive photostability of the Azurite variant has been attributed

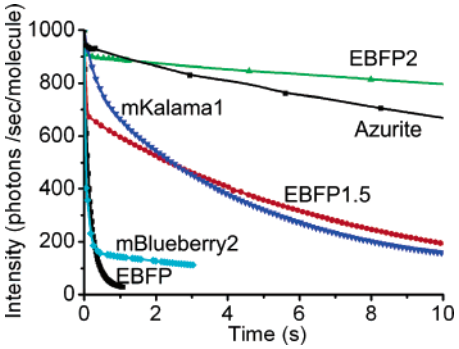

FIGURE 3: Photobleaching curves for the new blue-fluorescing FPs.

(Figure 3) (*12*). Azurite, EBFP1.5, and EBFP2 each display a biphasic rate of photobleaching in which the magnitude of the fast component increases with increasing intensity of illumination (data not shown). In contrast, mKalama1 displays a single exponential decrease in fluorescence intensity.

To determine whether the most promising of the new blue FPs were suitable for use in live cell fluorescence imaging, the genes encoding mKalama1, mBlueberry2, EBFP1.5, and EBFP2 were expressed in HeLa cells as a fusion with a nuclear localization sequence. A 6-fold longer exposure time was typically necessary to obtain satisfactory images of the bright but fast-bleaching mBlueberry2 variant. All of the new FPs correctly localized to the nucleus and did not exhibit significant fluorescence in the EGFP emission channel that was used for imaging of a cotransfected EGFP-actin fusion (Figure 4A−D). Blue FPs, such as the improved versions described in this manuscript, have excitation and emission maxima at wavelengths distinct from those of EGFP (excitation maxima at 488 nm and emission maximum at 507 nm) (*2*). However, because the absorbance profile of EGFP tails well below 400 nm, EGFP will fluoresce green with 10−20% of its maximum brightness when illuminated at wavelengths used for excitation of blue FPs (approximately 400 nm). This UV-excited fluorescence limits the utility of EGFP for multicolor imaging with the UV-excitable green variant T-Sapphire (excitation maxima at 399 nm and emission maximum at 511 nm) (*16*) but does not adversely affect multicolor imaging with blue FPs due to the distinctly different emission wavelengths.

Despite the fact that it has neither the highest intrinsic brightness nor the best photostability of the new variants (including Azurite), mKalama1 is the brightest blue FP when expressed in bacteria (Figure 4E−H). This result suggests that the intensive directed evolution effort that produced mKalama1 selected for efficient protein folding and chromophore maturation in bacteria in addition to high intrinsic brightness.

In conclusion, by exploring the potential of a variety of distinct FP chromophore structures, we have arrived at 3 new blue FPs (mKalama1, EBFP1.5, and EBFP2) that are vastly superior alternatives to EBFP. All 3 new FPs are also brighter than Azurite, but only EBFP2 has better photostability and is thus the blue FP of choice for use in live cell fluorescence imaging. For applications in which photostability is not particularly important, such as use as a reporter of gene expression in mammalian cells or bacterial colonies, mKalama1 may provide a higher fluorescent signal than EBFP2 due to its high folding and chromophore maturation efficiency.

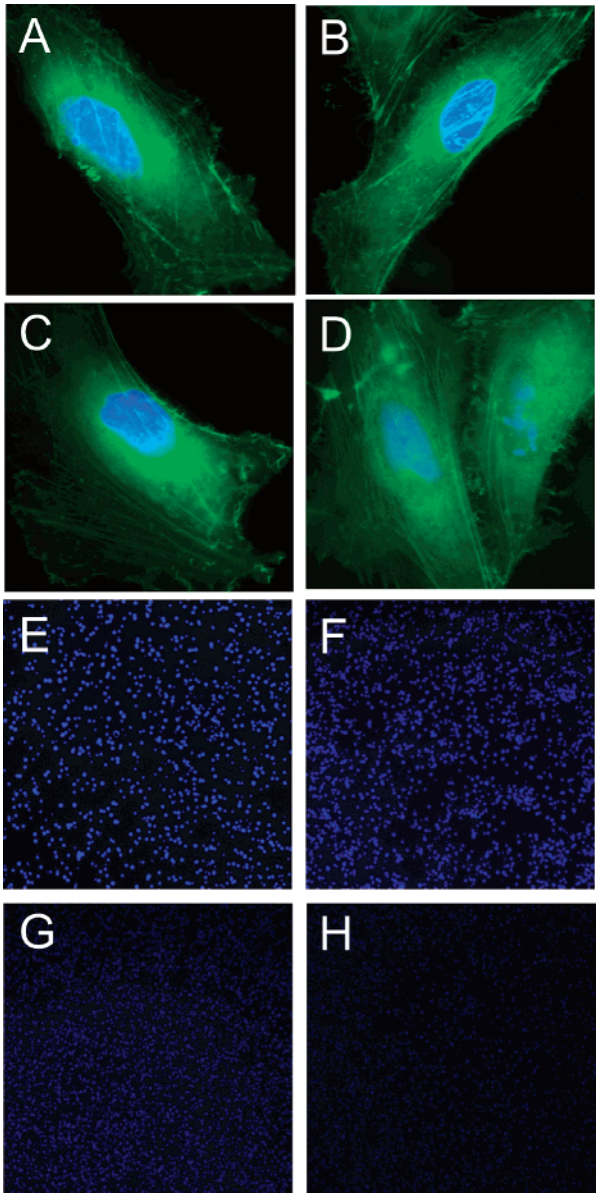

FIGURE 4: New blue-fluorescing FPs expressed in live cells. (A) mKalama1-NLS, (B) mBlueberry2-NLS, (C) EBFP1.5-NLS, or (D) EBFP2-NLS coexpressed with EGFP-actin in HeLa cells. Colonies of *E. coli* expressing either (E) mKalama1, (F) EBFP2, (G) Azurite, or (H) EBFP imaged 14 h after transformation and plating. Relative fluorescent intensities are 8, 5, 2, and 1, respectively. All plates were handled and imaged in parallel under identical conditions.

ACKNOWLEDGMENT

The authors thank the University of Alberta and the Canadian Foundation for Innovation for infrastructure support. R.E.C. holds a Canada Research Chair in Bioanalytical Chemistry. Anthony Lott, David Lin, and Marshall Yuan participated in this project as part of the Sanofi-Aventis Biotechnology Challenge.

REFERENCES

1. Tsien, R. Y. (1998) The green fluorescent protein, *Annu. Rev. Biochem. 67*, 509−544.
2. Shaner, N. C., Steinbach, P. A., and Tsien, R. Y. (2005) A guide to choosing fluorescent proteins, *Nat. Methods 2*, 905−909.

3. Heim, R., and Tsien, R. Y. (1996) Engineering green fluorescent protein for improved brightness, longer wavelengths and fluorescence resonance energy transfer, *Curr. Biol. 6*, 178−182.
4. Miyawaki, A., Nagai, T., and Mizuno, H. (2005) Engineering fluorescent proteins, *Adv. Biochem. Eng. Biotechnol. 95*, 1−15.
5. Ai, H. W., Henderson, J. N., Remington, S. J., and Campbell, R. E. (2006) Directed evolution of a monomeric, bright and photostable version of Clavularia cyan fluorescent protein: structural characterization and applications in fluorescence imaging, *Biochem. J. 400*, 531−540.
6. Shaner, N. C., Campbell, R. E., Steinbach, P. A., Giepmans, B. N., Palmer, A. E., and Tsien, R. Y. (2004) Improved monomeric red, orange and yellow fluorescent proteins derived from Discosoma sp. red fluorescent protein, *Nat. Biotechnol. 22*, 1567−1572.
7. Chalfie, M., Tu, Y., Euskirchen, G., Ward, W. W., and Prasher, D. C. (1994) Green fluorescent protein as a marker for gene expression, *Science 263*, 802−805.
8. Inouye, S., and Tsuji, F. I. (1994) Aequorea green fluorescent protein. Expression of the gene and fluorescence characteristics of the recombinant protein, *FEBS Lett. 341*, 277−280.
9. Wang, S., and Hazelrigg, T. (1994) Implications for bcd mRNA localization from spatial distribution of exu protein in Drosophila oogenesis, *Nature 369*, 400−403.
10. Heim, R., Prasher, D. C., and Tsien, R. Y. (1994) Wavelength mutations and posttranslational autoxidation of green fluorescent protein, *Proc. Natl. Acad. Sci. U.S.A. 91*, 12501−12504.
11. Yang, T. T., Sinai, P., Green, G., Kitts, P. A., Chen, Y. T., Lybarger, L., Chervenak, R., Patterson, G. H., Piston, D. W., and Kain, S. R. (1998) Improved fluorescence and dual color detection with enhanced blue and green variants of the green fluorescent protein, *J. Biol. Chem. 273*, 8212−8216.
12. Mena, M. A., Treynor, T. P., Mayo, S. L., and Daugherty, P. S. (2006) Blue fluorescent proteins with enhanced brightness and photostability from a structurally targeted library, *Nat. Biotechnol. 24*, 1569−1571.
13. Treynor, T. P., Vizcarra, C. L., Nedelcu, D., and Mayo, S. L. (2007) Computationally designed libraries of fluorescent proteins evaluated by preservation and diversity of function, *Proc. Natl. Acad. Sci. U.S.A. 104*, 48−53.
14. Cheng, Z., and Campbell, R. E. (2006) Assessing the structural stability of designed beta-hairpin peptides in the cytoplasm of live cells, *ChemBioChem 7*, 1147−1150.
15. Adams, M. J., Highfield, J. G., and Kirkbright, G. F. (1977) Determination of Absolute Fluorescence Quantum Efficiency of Quinine Bisulfate in Aqueous-Medium by Optoacoustic Spectrometry, *Anal. Chem. 49*, 1850−1852.
16. Zapata-Hommer, O., and Griesbeck, O. (2003) Efficiently folding and circularly permuted variants of the Sapphire mutant of GFP, *BMC Biotechnol. 3*, 5.
17. Dickson, R. M., Cubitt, A. B., Tsien, R. Y., and Moerner, W. E. (1997) On/off blinking and switching behaviour of single molecules of green fluorescent protein, *Nature 388*, 355−358.
18. Chudakov, D. M., Verkhusha, V. V., Staroverov, D. B., Souslova, E. A., Lukyanov, S., and Lukyanov, K. A. (2004) Photoswitchable cyan fluorescent protein for protein tracking, *Nat. Biotechnol. 22*, 1435−1439.
19. Zacharias, D. A., Violin, J. D., Newton, A. C., and Tsien, R. Y. (2002) Partitioning of lipid-modified monomeric GFPs into membrane microdomains of live cells, *Science 296*, 913−916.
20. Pedelacq, J. D., Cabantous, S., Tran, T., Terwilliger, T. C., and Waldo, G. S. (2006) Engineering and characterization of a superfolder green fluorescent protein, *Nat. Biotechnol. 24*, 79−88.
21. Matz, M. V., Fradkov, A. F., Labas, Y. A., Savitsky, A. P., Zaraisky, A. G., Markelov, M. L., and Lukyanov, S. A. (1999) Fluorescent proteins from nonbioluminescent Anthozoa species, *Nat. Biotechnol. 17*, 969−973.
22. Gross, L. A., Baird, G. S., Hoffman, R. C., Baldridge, K. K., and Tsien, R. Y. (2000) The structure of the chromophore within DsRed, a red fluorescent protein from coral, *Proc. Natl. Acad. Sci. U.S.A. 97*, 11990−11995.
23. Wachter, R. M., King, B. A., Heim, R., Kallio, K., Tsien, R. Y., Boxer, S. G., and Remington, S. J. (1997) Crystal structure and photodynamic behavior of the blue emission variant Y66H/Y145F of green fluorescent protein, *Biochemistry 36*, 9759−9765.
24. Shimomura, O. (1979) Structure of the Chromophore of Aequorea Green Fluorescent Protein, *FEBS Lett. 104*, 220−222.
25. Heim, R., Cubitt, A. B., and Tsien, R. Y. (1995) Improved green fluorescence, *Nature 373*, 663−664.
26. Kogure, T., Karasawa, S., Araki, T., Saito, K., Kinjo, M., and Miyawaki, A. (2006) A fluorescent variant of a protein from the stony coral Montipora facilitates dual-color single-laser fluorescence cross-correlation spectroscopy, *Nat. Biotechnol. 24*, 577−581.

BI700199G